Physica A 390 (2011) 4045–4055

Contents lists available at SciVerse ScienceDirect

Physica A

journal homepage: www.elsevier.com/locate/physa

Controlling statistical properties of a Cooper pair box interacting with a nanomechanical resonator

C. Valverde [a,b,c,*], A.T. Avelar [c], B. Baseia [c]

[a] Universidade Paulista, Rod. BR 153, km 7, 74845-090 Goiânia, GO, Brazil

[b] Universidade Estadual de Goiás, Rod. BR 153, 3105, 75132-903 Anápolis, GO, Brazil

[c] Instituto de Física, Universidade Federal de Goiás, 74001-970 Goiânia, GO, Brazil

ARTICLE INFO

Article history:
Received 15 April 2011
Received in revised form 7 June 2011
Available online 5 July 2011

Keywords:
Quantum entropy
Power spectrum
Excitation inversion
Cooper pair box
Nanomechanical resonator

ABSTRACT

We investigate the quantum entropy, its power spectrum, and the excitation inversion of a Cooper pair box interacting with a nanomechanical resonator, the first initially prepared in its excited state, the second prepared in a "Schrödinger-cat" state. The method employs the Jaynes–Cummings model with damping, with different decay rates of the Cooper pair box and different ranges of detuning, going from resonant to off-resonant cases, including time dependent detunings. Concerning the entropy, it is found that the time dependent detuning turns the entanglement more stable in comparison with previous results in the literature. With respect to the Cooper pair box excitation inversion, while the presence of detuning destroys the collapses and revivals, it is shown that convenient time dependent detunings recover such effects in a nice way.

1. Introduction

In the past years, there has been great interest in producing new nonclassical states of quantized electromagnetic field, one of several interesting topics of Quantum Optics. In spite of the quantized field in 1925, the quantum optical effects were observed only seven decades later, the first of them being the antibunching effect, as predicted by Carmichael and Walls in 1976 [1], experimentally confirmed by the group of Kimble [2] in 1977. A second nonclassic optical effect was observed in 1985 in Ref. [3], theoretically anticipated in Ref. [4] in 1970. A third one, oscillations in the photon statistical distribution, was observed in 1987 in Ref. [5]. Since then, various nonclassical states of the quantized electromagnetic field were studied, including their practical realization in laboratories in different systems—one of them being the celebrated "Schrödinger-cat" (SC) state, whose generation was first suggested in Ref. [6], the pioneer experimental observation being obtained by the group of Haroche [7]. More recently, the community became aware of the experimental observation of the decoherence of the SC state, in both domains: in optical [8] and atomic physics [9], constituting the first observation of the passage through the frontier that separates the quantum and classical realms. After this, another interesting topic emerged in the literature, as the quantum teleportation of states, first suggested in Ref. [10], based on the nonlocal character of quantum mechanics and contextualized by the EPR entangled states [11]. This somewhat "bizarre" effect was first observed experimentally in 1997, by the group of Zeilinger [12], concerned with the teleportation of a single photon state; the effect was later extended for atomic states and also for a huge quantity of photons [13]. Then, several publications in this line appeared in the literature [14–17].

Besides the nonclassical effects exhibited by the light field states, many researchers became interested in the study of new states and new effects they could exhibit, mainly concerned with their potential applications [18]. Then, the study of

* Corresponding author at: Universidade Paulista, Rod. BR 153, km 7, 74845-090 Goiânia, GO, Brazil. Tel.: +55 06284081336.
E-mail address: valverde@unip.br (C. Valverde).

0378-4371
doi:10.1016/j.physa.2011.06.007

various schemes for the generation of nonclassical states of the light field became also interesting [19–21]. To this end, two lines of study emerged: (i) when the issue is concerned with a state of a stationary field, inside a high-Q microwave cavity; (ii) when it is concerned with traveling fields, either throughout the free space or a medium (optical fibers, beam splitters, prisms, etc.). In both cases various proposals appeared in literature [22–25]. The extension of these investigations for atomic systems has also been implemented. In this case the system consists of atoms, either located inside a cavity or crossing it, including atoms trapped inside magneto-optical devices [26,27].

When focusing either the field or atomic cases the theoretical strategy starts from a Hamiltonian describing the atom–field system, traditionally treated via the Jaynes–Cummings model and usually assuming the atom–field coupling as a constant parameter. The number of works in the literature using such assumption is vastly larger in comparison with the case of atom–field coupling and/or the atomic frequency assumed as a time dependent parameter [28–32], including the case of time dependent amplitude [33]. Nevertheless, this scenario is also relevant. For example, the state of two qubits (qubits stand for quantum bits) with a desired degree of entanglement can be generated via a time dependent atom–field coupling [34]; such coupling can modify the dynamical properties of the atom and field, with transitions that involve a large number of photons [35]. In general, these studies are simplified by neglecting the atomic decay from an excited level. Theoretical treatments taking into account this complication of the real world may also use an adapted Jaynes–Cummings model. In these case, as expected, one observe decoherence of the state describing the system, since the presence of dissipation destroys the state of a system as time flows.

Here, taking advantage of what we have learned about the atom–field interaction, we will study an advantageous system in practice (due to its rapid response and better controllability [36]) by considering a nanomechanical resonator (NR) that interacts with a Cooper pair box (CPB). This nanodevice has its own interest since its macroscopic nature and peculiar effect of low-frequency noise in the solid-state impose obstacles requiring more careful studies than a mere translation from quantum optics. It has been explored in the study of quantum nondemolition measurements [37,38], in the study of decoherence of nonclassical states, as Fock states and superposition or entangled states describing mesoscopic systems [39], etc. The fast advance in the technique of fabrication in nanotechnology implied great interest in the study of the NR system in view of its potential modern applications, as a sensor, largely used in various domains, as in biology, astronomy, quantum computation, and more recently in quantum information [40] to implement the quantum qubit [41] and the production of nonclassical states, e.g.: Fock states [42], "Schrödinger-cat" states [43], squeezed states [44], clusters states [45], etc. In particular, when accompanied by superconducting charge qubits the NR has been used to prepare entangled states [46]. For example, Zhou et al. [44] have proposed a scheme to prepare squeezed states using a NR coupled to a CPB qubit; in this proposal the NR–CPB coupling is under an external control while the connection between these two interacting subsystems play an important role in quantum computation. Such a control is achieved via convenient change of system parameters, which can set "*on*" and "*off*" the interaction between the NR and the CPB, on demand.

One of the desired goals in this report is to verify the behavior and properties of an entangled state describing the CPB–NR system, via the Jaynes–Cummings model, by considering the energy dissipation in the CPB during its transitions from an excited level to a ground state. Another target is to verify if, and in which way, the time dependence of the CPB–NR coupling modifies the dynamical properties of the state describing a subsystem. We will also study the time evolution of the quantum entropy and its power spectrum, as well as the CPB excitation inversion. There are some evidences of entropy production, including the fact that the power spectrum of stationary systems and subsystems can be used as dynamical criteria for quantum chaos [47,48]. For the entropy power spectrum, such criteria embody those already discussed in the literature concerned with fixed parameters. Then, it seems adequate to look at the various characteristics of the entropy to formulate a reasonable and sufficient universal dynamical criterion for the quantum chaos. The degree of entanglement, represented by the entropy in certain circumstances, has also shown itself being sensible to the presence of a classical chaos [49,50].

2. Model Hamiltonian for the CPB–NR system

There exist in the literature a large number of devices using the SQUID-base, where the CPB charge qubit consists of two superconducting Josephson junctions in a loop. In the present model a CPB is coupled to a NR as shown in Fig. 1. The scheme is inspired by the works of Jie-Qiao Liao et al. [41] and Zhou et al. [44] where we have substituted each Josephson junction by two of them. This creates a new configuration that includes a third loop. A superconducting CPB charge qubit is adjusted via a voltage V_1 at the system input and a capacitance C_1. We want the scheme attaining an efficient tunneling effect for the Josephson energy. In Fig. 1 we observe three loops: one great loop between two small ones. This makes it easier to control the external parameters of the system since the control mechanism includes the input voltage V_1 plus three external fluxes Φ_L, Φ_r and $\Phi_e(t)$. In this way one can induce small neighboring loops in the nanodevice. The great loop contains the NR and its effective area in the center of the apparatus changes as the NR oscillates, which creates an external flux $\Phi_e(t)$ that provides the CPB–NR coupling to the system. In this work we will assume the four Josephson junctions being identical, with the same Josephson energy E_J^0, the same being assumed for the external fluxes Φ_L and Φ_r, i.e., with same magnitude, but opposite sign: $\Phi_L = -\Phi_r = \Phi_x$. In this way, we can write the Hamiltonian describing the entire system as

$$\hat{H} = \omega \hat{a}^\dagger \hat{a} + 4E_c \left(N_1 - \frac{1}{2}\right) \hat{\sigma}_z - 4E_J^0 \cos\left(\frac{\pi \Phi_x}{\Phi_0}\right) \cos\left(\frac{\pi \Phi_e}{\Phi_0}\right) \hat{\sigma}_x, \tag{1}$$

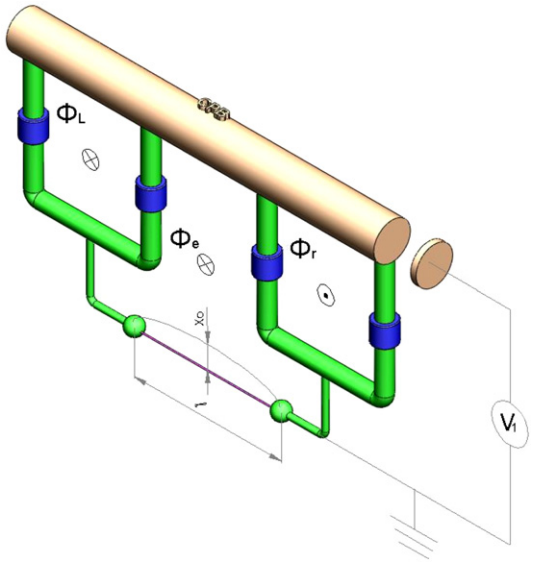

Fig. 1. Model for the CPB–NMR coupling.

where $\hat{a}^\dagger(\hat{a})$ is the creation (annihilation) operator for the excitation in the NR, corresponding to the frequency ω and mass m; E_J^0 and E_c are respectively the energy of each Josephson junction and the charge energy of a single electron. The parameters C_1 and C_J^0 stand for the input capacitance and the capacitance of each Josephson tunnel, respectively. $\Phi_0 = h/2e$ is the quantum flux and $N_1 = C_1V_1/2e$ is the charge number in the input with the input voltage V_1. We have used the Pauli matrices to describe our system operators, where the states $|g\rangle$ and $|e\rangle$ (or 0 and 1) represent the number of extra Cooper pairs in the superconduction island. We have: $\hat{\sigma}_z = |g\rangle\langle g| - |e\rangle\langle e|$, $\hat{\sigma}_x = |g\rangle\langle e| - |e\rangle\langle g|$ and $E_C = e^2/(C_1 + 4C_J^0)$.

The magnetic flux can be written as the sum of two terms,

$$\Phi_e = \Phi_b + B\ell\hat{x}, \tag{2}$$

where the first term Φ_b is the induced flux, corresponding to the equilibrium position of the NR and the second term describes the contribution due to the vibration of the NR; B represents the magnetic field created in the loop. We have assumed the displacement $\hat{x}$ described as $\hat{x} = x_0(\hat{a}^\dagger + \hat{a})$, where $x_0 = \sqrt{m\omega/2}$ represents the amplitude of oscillation. Substituting the Eq. (2) in Eq. (1) and controlling the flux Φ_b to adjust $\cos\left(\frac{\pi\Phi_b}{\Phi_0}\right) = 0$ we obtain

$$\hat{H} = \omega\hat{a}^\dagger\hat{a} + 4E_c\left(N_1 - \frac{1}{2}\right)\hat{\sigma}_z - 4E_J^0\cos\left(\frac{\pi\Phi_x}{\Phi_0}\right)\sin\left(\frac{\pi B\ell\hat{x}}{\Phi_0}\right)\hat{\sigma}_x. \tag{3}$$

The approximation $\pi B\ell x/\Phi_0 \ll 1$ leads the foregoing equation to simplified form

$$\hat{H} = \omega\hat{a}^\dagger\hat{a} + \frac{1}{2}\omega_0\hat{\sigma}_z + \lambda_0(\hat{a}^\dagger + \hat{a})\hat{\sigma}_x, \tag{4}$$

where λ_0 stands for the CPB–NR coupling, $\lambda_0 = -4E_J^0\cos\left(\frac{\pi\Phi_x}{\Phi_0}\right)\left(\frac{\pi B\ell x_0}{\Phi_0}\right)$ whereas $\omega_0 = 8Ec(N_1 - \frac{1}{2})$ is the effective energy standing for the transition frequency of the CPB. In the rotating wave approximation the Hamiltonian given in Eq. (4) becomes

$$\hat{H} = \omega\hat{a}^\dagger\hat{a} + \frac{1}{2}\omega_0\hat{\sigma}_z + \lambda_0(\hat{\sigma}_+\hat{a} + \hat{a}^\dagger\hat{\sigma}_-). \tag{5}$$

Next, we consider a more general scenario by substituting $\omega \to \omega(t) = \omega + f(t)$ and $\lambda_0 \to \lambda(t) = \lambda_0[1 + f(t)/\omega]$ [35,51]. In addition we assume the presence of a constant decay rate γ in the CPB, from its excited level to the ground state. $\hat{\sigma}_\pm$ and $\hat{\sigma}_z$ stand for CPB transition and excitation inversion operators, respectively. They act on the Hilbert space of atomic states and satisfy the commutation relations $\left[\hat{\sigma}_+, \hat{\sigma}_-\right] = \hat{\sigma}_z$ and $\left[\hat{\sigma}_z, \hat{\sigma}_\pm\right] = \pm\hat{\sigma}_\pm$. As well known, the coupling parameter $\lambda(t)$ is proportional to $\sqrt{\omega(t)/V(t)}$, where the time dependent quantization volume $V(t)$ takes the form $V(t) = V_0/[1 + f(t)/\omega]$ [52,31,51]. Accordingly, we obtain the new (Non-Hermitian) Hamiltonian

$$\hat{H} = \omega(t)\hat{a}^\dagger\hat{a} + \frac{1}{2}\omega_0\hat{\sigma}_z + \lambda(t)(\hat{\sigma}_+\hat{a} + \hat{a}^\dagger\hat{\sigma}_-) - i\frac{\gamma}{2}|e\rangle\langle e|. \tag{6}$$

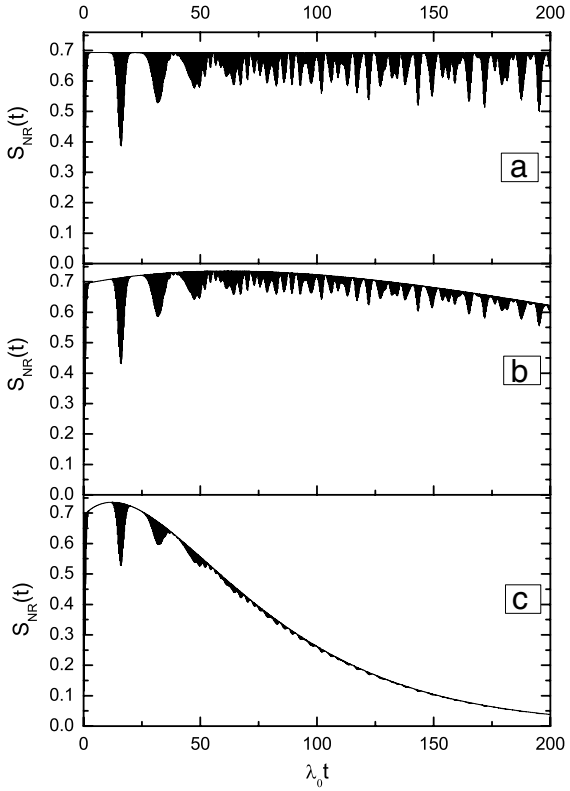

Fig. 2. Time evolution of the Entropy when the NR is initially prepared in an even "cat state", for different values of the decay rate γ: (a) $\gamma = 0.0\lambda_0$, (b) $\gamma = 0.01\lambda_0$, and (c) $\gamma = 0.05\lambda_0$, with $\alpha = 5$, $\omega = \omega_0 = 2000\lambda_0$, $f(t) = 0$.

Non-Hermitian Hamiltonians (NHH) have been used widely in the literature. To mention some few examples: Ref. [53], where the authors use a NHH and an algorithm to generalize the conventional theory; Ref. [54], using a NHH to get information about entrance and exit channels; Ref. [55], using non-Hermitian techniques to study canonical transformations in quantum mechanics; Ref. [56], solving quantum master equations in terms of NHH; Ref. [57], using a new approach for NHH to study the spectral density of weak H-bonds involving damping; Ref. [58], studying NHH with real eigenvalues; Ref. [59], using a canonical formulation to study dissipative mechanics exhibiting complex eigenvalues; Ref. [60], studying NHH in non-commutative spaces, and more recently: Ref. [61], studying the optical realization of relativistic NHH; Ref. [31], studying the evolution of entropy of atom–field interaction; Ref. [30], including damping in a JC-Model to study entanglement between two atoms, each of them within distinct cavities.

3. Solving the CPB–NR system

Now, the state describing our time dependent system can be written as

$$|\Psi(t)\rangle = \sum_{n=0}^{\infty} (C_{g,n}(t)|g, n\rangle + C_{e,n}(t)|e, n\rangle). \tag{7}$$

Taking the CPB initially prepared in its excited state $|e\rangle$ and the NR in a superposition of two coherent states, $|\beta\rangle = \eta(|\alpha\rangle + |-\alpha\rangle)$, and expanding each coherent state component in the Fock basis, i.e., $|\alpha\rangle = \exp(-|\alpha|^2/2) \sum_{n=0}^{\infty} (\alpha^n/\sqrt{n!})|n\rangle$, we obtain $|\beta\rangle = \sum_{n=0}^{\infty} F_n|n\rangle$ where $\eta = [2 + 2\exp(-2\alpha^2)]^{-1/2}$ is a normalization factor. Assuming the NR and CPB decoupled at $t = 0$ and the initial conditions $C_{g,n}(0) = 0$ and $\sum_{n=0}^{\infty} \left|C_{e,n}(0)\right|^2 = 1$ we may write the Eq. (7) as

$$|\Psi(0)\rangle = \sum_{n=0}^{\infty} F_n|e, n\rangle. \tag{8}$$

The time dependent Schrödinger equation for the present system is

$$\mathrm{i}\frac{\mathrm{d}|\Psi(t)\rangle}{\mathrm{d}t} = \hat{H}|\Psi(t)\rangle, \tag{9}$$

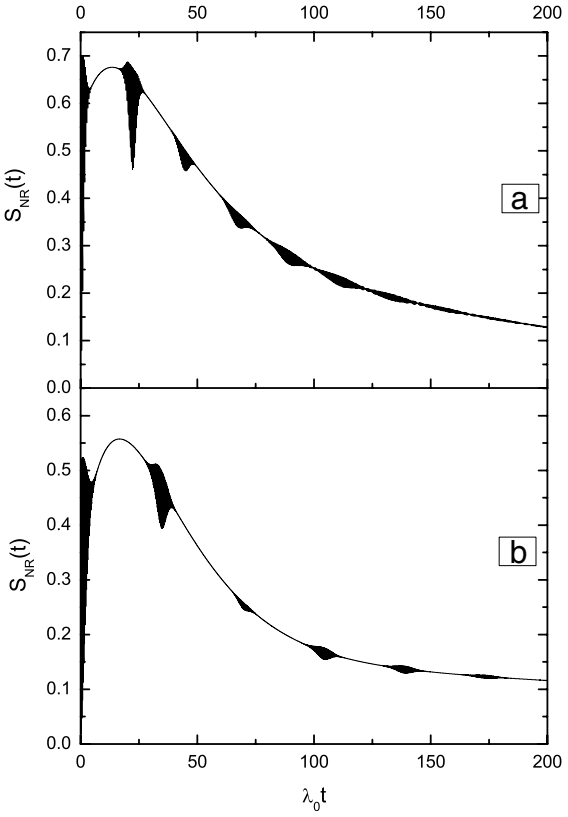

Fig. 3. Same as in Fig. 2, now for different values of detunings (cf. $f(t) = \Delta = \text{const}$): (a) $\Delta = 10\lambda_0$ and (b) $\Delta = 20\lambda_0$, with $\alpha = 5, \omega = \omega_0 = 2000\lambda_0, \gamma = 0.05\lambda_0$.

with the Hamiltonian $\hat{H}$ given in Eq. (6). Substituting Eq. (6) in Eq. (9) we get the (coupled) equations of motion for the probability amplitudes $C_{e,n}(t)$ and $C_{g,n+1}(t)$,

$$\frac{\partial C_{e,n}(t)}{\partial t} = -\mathrm{i}n\omega(t)C_{e,n}(t) - \frac{\mathrm{i}}{2}\omega_0 C_{e,n}(t) - \mathrm{i}\lambda(t)\sqrt{n+1}C_{g,n+1}(t) - \frac{\gamma}{2}C_{e,n}(t), \tag{10}$$

$$\frac{\partial C_{g,n+1}(t)}{\partial t} = -\mathrm{i}(n+1)\omega(t)C_{g,n+1}(t) + \frac{\mathrm{i}}{2}\omega_0 C_{g,n+1}(t) - \mathrm{i}\lambda(t)\sqrt{n+1}C_{e,n}(t). \tag{11}$$

The solutions of the coefficients $C_{e,n}(t)$, $C_{g,n+1}(t)$ furnish the quantum dynamical properties of the system, including the CPB–NR entanglement. For the cases $f(t) = 0$ and $f(t) = \text{const.}$, the solution of the system of equations Eqs. (10) and (11) is obtained exactly. We find, analytically,

$$C_{g,n+1}(t) = (1/\zeta)[-2\mathrm{i}\lambda \mathrm{e}^{-1/4\delta t}\left(\mathrm{e}^{1/4\zeta t} - \mathrm{e}^{-1/4\zeta t}\right)\sqrt{n+1}F_n], \tag{12}$$

$$C_{e,n}(t) = (1/2\zeta)\,[\mathrm{i}\mathrm{e}^{-1/4\delta t}\left(\mathrm{e}^{1/4\zeta t}\left(\mathrm{i}\gamma + 2\omega - \mathrm{i}\zeta - 2\omega_0\right) - \mathrm{e}^{-1/4\zeta t}\left(\mathrm{i}\gamma + 2\omega + \mathrm{i}\zeta - 2\omega_0\right)\right)F_n], \tag{13}$$

where $\delta = \gamma + 2\mathrm{i}\omega(1+2n)$ and $\zeta = [\gamma(\gamma + 4\mathrm{i}(\omega_0 - \omega)) - 4(\omega^2 + \omega_0^2) - 16\lambda^2(1+n) + 8\omega\omega_0]^{1/2}$. However, when the coupling $f(t)$ is time dependent the solution of this system of equations is found only numerically. As well known, in the presence of decay rate γ in the CPB the state of the whole CPB–NR system becomes mixed. In this case its description requires the use of the density operator $\hat{\rho}_{CN}$, which describes the entire system. To obtain the reduced density operator that describes the CPB (NR) subsystem we must trace over variables of the NR (CPB) subsystem. For example,

$$\hat{\rho}_{\mathrm{NR}} = \mathrm{Tr}_{\mathrm{CPB}}(\hat{\rho}_{CN}) = \sum_n \sum_{n'} \left[C_{e,n}(t)C^*_{e,n'}(t) + C_{g,n}(t)C^*_{g,n'}(t)\right]|n\rangle\langle n'|. \tag{14}$$

4. Entropy of subsystems

Recently, researchers have employed several methods to study the dynamical of entanglement [30–32,62,63]. As proved in Ref. [64] the von Neumann entropy offers a quantitative measure of disorder of a system and of the purity of a quantum state. Such entropy, defined as $S_{\mathrm{NR}(C)} = -\mathrm{Tr}(\hat{\rho}_{N(C)} \ln \hat{\rho}_{N(C)})$, is a measure that is sensible to quantum entanglement of

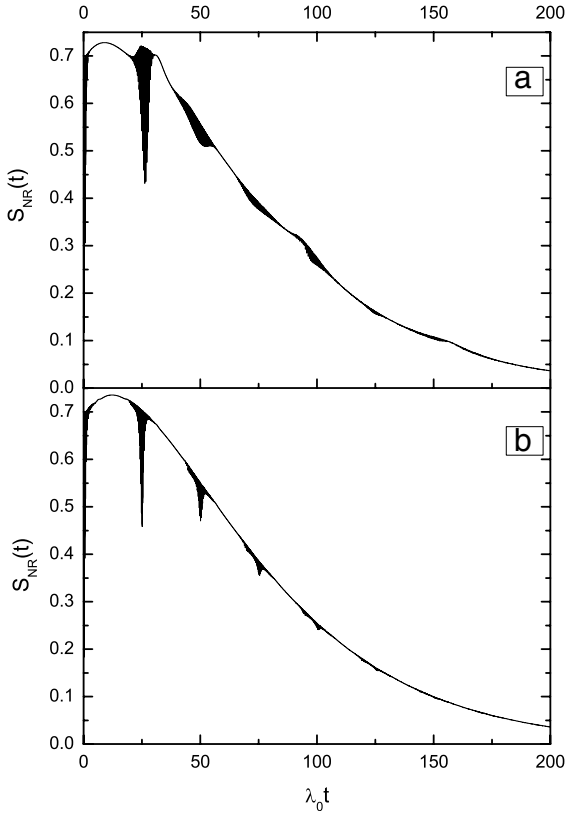

Fig. 4. Same as in Figs. 2 and 3, for time dependent detunings (cf. $f(t) = c\,\sin(\omega' t)$): with (a) $c = 20\lambda_0 e\omega' = 0.1\lambda_0$, and (b) $c = 20\lambda_0 e\omega' = 0.5\lambda_0$.

two interacting subsystems. The quantum dynamics described by the Eq. (6) furnishes the CPB–NR entanglement and we will employ the von Neumann quantum entropy as a measure of the degree of entanglement. The entropy S of a quantum system, when composed of two subsystems, obeys a theorem due to Araki and Lieb, which establishes that: $|S_{\rm CPB} - S_{\rm NR}| \leq S \leq S_{\rm CPB} + S_{\rm NR}$; $S_{\rm CPB}$ with $S_{\rm NR}$ standing for the entropies of the NR subsystems. S stands for the total entropy of the CPB–NR system. One immediate consequence of the above inequality is that, if one prepares the entire system in a pure state at $t = 0$, then both components of the whole system have the same entropy for the subsequent time evolution. So, when assuming our system initially in a pure and decoupled state the entropies of the CPB and NR become identical, namely, $S_{\rm CPB}(t) = S_{\rm NR}(t)$. Then, one only needs to calculate the quantum entropy of one subsystem to get its entanglement evolution. We obtain, from the Eq. (14) and $S_{\rm NR} = -{\rm Tr}(\hat{\rho}_{\rm NR} \ln \hat{\rho}_{\rm NR})$,

$$S_{\rm NR}(t) = -\left[\wedge^{+}_{\rm NR}(t) \ln(\wedge^{+}_{\rm NR}(t)) + \wedge^{-}_{\rm NR}(t) \ln(\wedge^{-}_{\rm NR}(t))\right], \tag{15}$$

where,

$$\wedge^{\pm}_{\rm NR}(t) = \frac{1}{2}\left(1 \pm \sqrt{(\langle R_1|R_1\rangle - \langle R_2|R_2\rangle)^2 + 4\,|\langle R_1|R_2\rangle|^2}\right), \tag{16}$$

with $\langle R_1|R_1\rangle = \sum_{n=0}^{\infty} \left|C_{e,n}(t)\right|^2$, $\langle R_2|R_2\rangle = \sum_{n=0}^{\infty} \left|C_{g,n+1}(t)\right|^2$ and $\langle R_1|R_2\rangle = \langle R_2|R_1\rangle^* = \sum_{n=0}^{\infty} C^*_{e,n+1}(t) C_{g,n+1}(t)$.

We can now look at the time evolution of the NR entropy. We will assume the NR subsystem initially in an even "SC" state, $|\beta\rangle = \eta(|\alpha\rangle + |-\alpha\rangle)$. Firstly we consider the resonant case ($f(t) = 0$) and we look for the time evolution of the NR entropy with different decay rates γ in the CPB, with $\omega = \omega_0 = 2000\lambda_0$ and the NR state with $\alpha = 5$, as shown in Fig. 2(a), (b), and (c). In an ideal case the CPB decay rate vanishes. As displayed in Fig. 2(a) the maximum value of the entropy of the NR is close to $\ln 2$. Just after the start of the CPB–NR interaction the entropy of the NR stabilizes at this value by a small interval and then recovers the oscillations as time goes on. The CPB subsystem is stable while standing in its ground state $|g\rangle$; but when lying in its excited state $|e\rangle$ various factors as spontaneous emission among others imply its decay to the ground state. For a small decay rate (see Fig. 2(b)) the maximum entanglement becomes significant only for large times. However, the increase of the decay rate produces a drastic change on the entanglement (see Fig. 2(c)), with large reductions in their swings, which leads the CPB to its ground state (zero entropy). This effect upon the entropy of the CPB also affects the entropy of the NR (Fig. 2). Secondly, we modify the previous case by including the presence of detuning ($f(t) = \Delta \neq 0$) to verify its influence upon our interacting system. We take the decay rate as $\gamma = 0.05\lambda_0$, with $f(t) = \Delta = $ const and

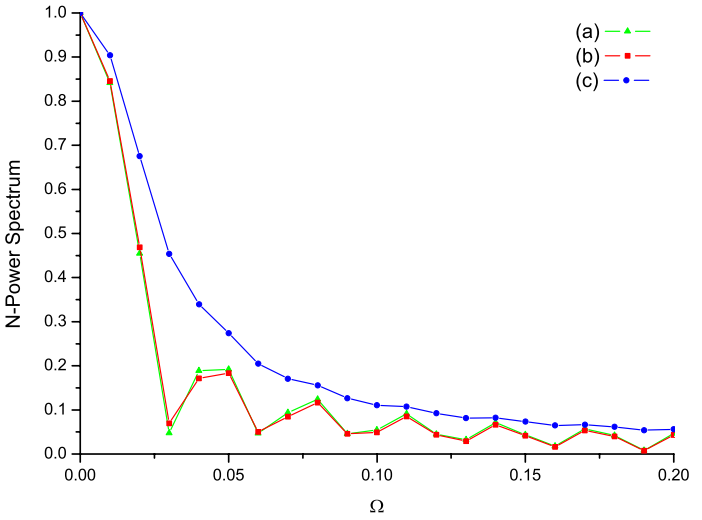

Fig. 5. Time evolution of the Normalized Power Spectrum when the NR is initially prepared in "cat state", concerning with the Entropies shown in the plots of Fig. 2: the plot 5(i) refers to the plot 2(i), $i = a, b, c$.

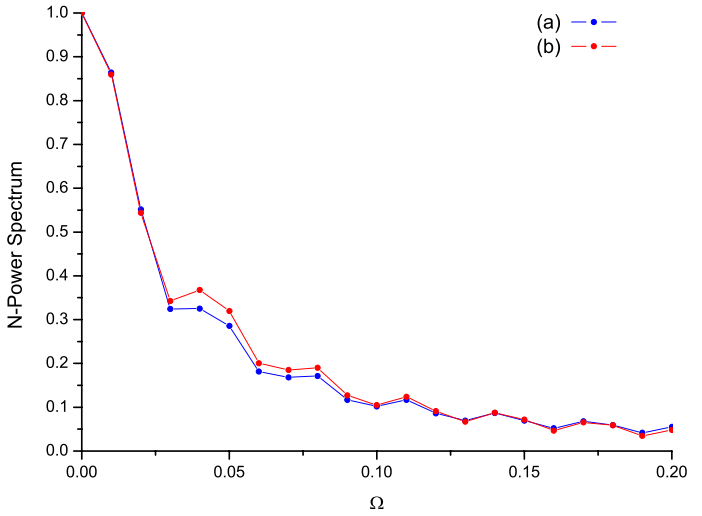

Fig. 6. Same as in Fig. 5, concerning with the Entropies shown in the plots of Fig. 3: the plot 6(i) refers to the plot 3(i), $i = a, b$.

$\Delta \ll \omega_0, \omega$. As result the entanglement remains for long time as the value of Δ increases, as we see comparing Fig. 3(a) with Fig. 2(c); this event is accompanied by a diminution of the maximum entropy (see Fig. 3(a) and (b)). When the detuning increases, the CPB transitions decreases (cf. Fig. 9).

Thirdly, we extend the detuning to the time dependent case, assuming $f(t) = c\,\sin(\omega' t)$, where c and ω' are parameters of amplitude and frequency modulation of the NR with the condition $\omega' < c \ll \omega_0, \omega$. Comparing the Fig. 4(a) with Fig. 3(b) we see that the sinusoidal modulation does not favor the entanglement for long time. However, the frequency modulation increases the maximum entanglement (see Fig. 4). Comparing Fig. 4(a) with Fig. 4(b) we see that when the frequency ω' grows the oscillations of entropy decrease.

5. Power spectrum of the entropy

To get a better understanding of the entropy we have considered its power spectrum (PS). It consists of a frequency dependent function, being real, positive, and constructed from the following Fourier transform [52]

$$PS(\varpi) = \frac{1}{\pi}\int_0^{\tau_{\max}} S_{\mathrm{NR}}(t)\,\exp(\mathrm{i}\varpi t)\mathrm{d}t, \tag{17}$$

where $\tau_{\max} = \lambda_0 t_{\max}$ stands for the maximum interaction interval in the plot $S_{\mathrm{NR}}(t)$ versus $\lambda_0 t$.

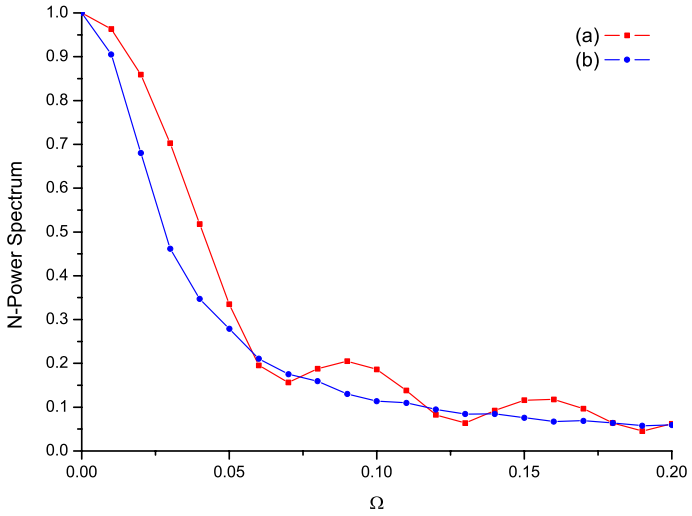

Fig. 7. Same as in Figs. 5 and 6, concerning with the Entropies shown in the plots of Fig. 4: the plot 7(i) refers to the plot 4(i), $i = a, b$.

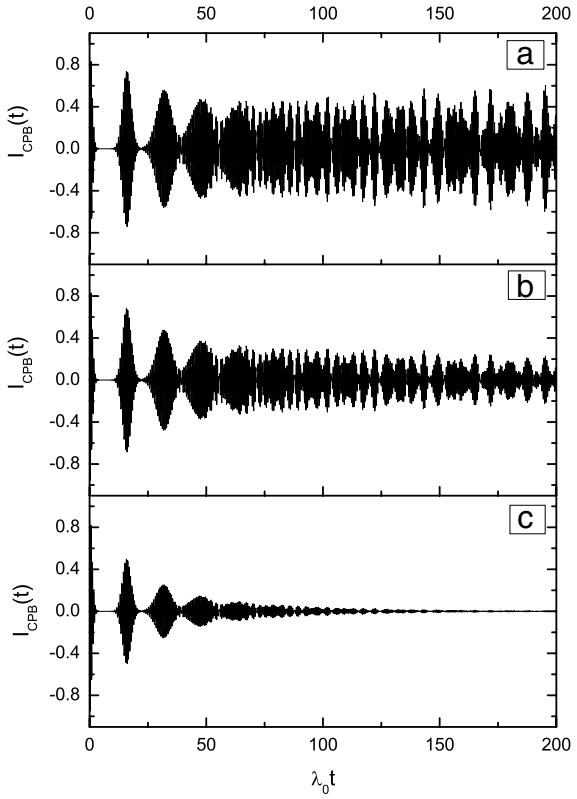

Fig. 8. Time evolution of the CPB Excitation Inversion with the NR initially prepared in the even "cat state", for various values of the decay rate: (a) $\gamma = 0.0\lambda_0$ (b) $\gamma = 0.01\lambda_0$, and (c) $\gamma = 0.05\lambda_0$, with $\alpha = 5$, $\omega = \omega_0 = 2000\lambda_0$, and $f(t) = 0$ (resonance).

The entropy PS is obtained from the above equation, as displayed in Fig. 2(a), (b) and (c). As expected, the amplitude of oscillations of this PS is reduced in the presence of growing decay rates (see Fig. 5(a), (b) and (c)); when we add a constant detuning ($f(t) = \Delta \neq 0$) and a decay rate $\gamma = 0.05\lambda_0$ we see in Fig. 6(a) and (b) the maximum value of the PS increasing when Δ also increases. In the case $f(t) = c\sin(\omega' t)$ the frequency of entropy PS is smoothly attenuated, with a peak around $\Omega = 0.1$, as shown in Fig. 7(a). When the frequency ω' increases the entropy PS is rapidly attenuated (cf. Fig. 7(a) and (b)).

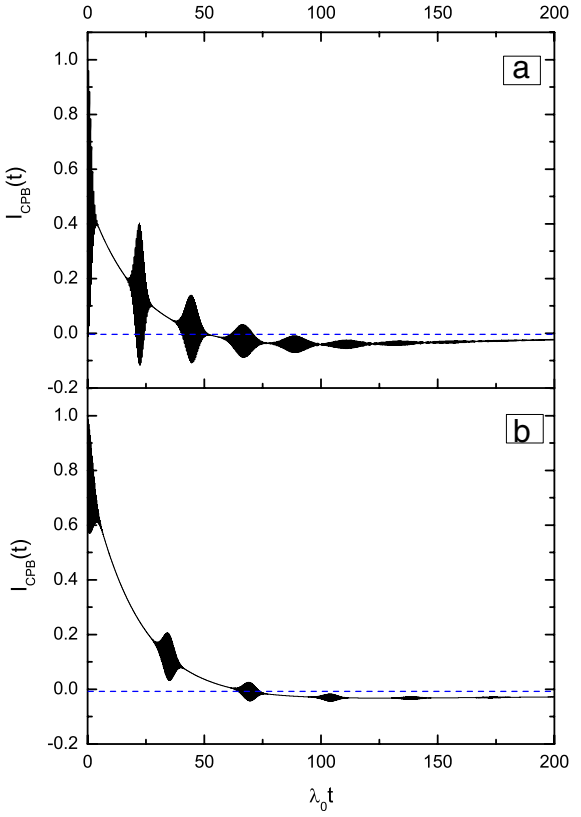

Fig. 9. Same as in Fig. 8, for different values of detuning (cf. $f(t) = \Delta = \text{const}$): (a) $\Delta = 10\lambda_0$ and (b) $\Delta = 20\lambda_0$, with $\alpha = 5$, $\omega = \omega_0 = 2000\lambda_0$, $\gamma = 0.05\lambda_0$.

6. Excitation inversion of the CPB

The CPB excitation inversion, $I_{\text{CPB}}(t)$, is an important observable of two level systems. It is defined as the difference of the probabilities of finding the system in the excited and in the ground state. For the CPB it reads,

$$I_{\text{CPB}}(t) = \sum_{n=0}^{\infty} \left[|C_{e,n}(t)|^2 - |C_{g,n+1}(t)|^2 \right]. \tag{18}$$

The Eq. (18) allows us to find the time evolution of the CPB excitation inversion. First, we assume the resonant case ($f(t) = 0$), for different values of the decay rate γ, with $\alpha = 5$ and $\omega = \omega_0 = 2000\lambda_0$ as in Fig. 8. Fig. 8(a)–(c) exhibit identical collapse and revival, but with different amplitudes: the higher the decay rate, the lower the amplitude of oscillations of the CPB excitation inversion. However, in the presence of a fixed detuning, with $f(t) = \Delta = \text{const}$ and $\Delta \ll \omega_0, \omega$, we see that the CPB excitation inversion in Fig. 9(a) occurs only inside the interval $\tau = \lambda_0 t \in (15, 30)$; differently, in Fig. 9(b) this event occurs inside the interval $\tau \in (50, 75)$, with amplitude smaller than that in Fig. 9(a); this is the effect caused by a constant detuning upon the CPB excitation inversion.

For a time dependent detuning, $f(t) = c\sin(\omega' t)$, the frequency of the CPB excitation inversion accompanies the frequency ω', as shown in Fig. 10. When we compare the Fig. 10(b) with Fig. 8(c), we see: if ω' increases, the interval of collapse of the excitation inversion also increases. However, looking at Fig. 10(a), (b) we see that the increasing of ω' as in Fig. 10(b) introduces equally spaced collapse intervals, accompanied by revivals modulated by the parameter ω'. Now, we can compare the CPB excitation inversion obtained with constant detuning ($f(t) = \Delta = \text{const}$) and that obtained with a time dependent detuning ($f(t) = c\sin(\omega' t)$): looking at Fig. 9 we see the plots of excitation inversion showing neither collapses nor revivals, with exceptions of small regions exhibiting excitation inversion (Fig. 9(a)); in Fig. 9(b) only a single such region appears. However, when considering the time dependent detuning (Fig. 10(b)), we see it nicely restituting those collapses and revivals that appear in the resonant case (cf. Fig. 8(c)).

7. Conclusion

We have considered a Hamiltonian model for a CPB–NR interacting system to study entropy, its power spectrum and the CPB excitation inversion. These properties characterize the entangled state that describes this coupled system for various

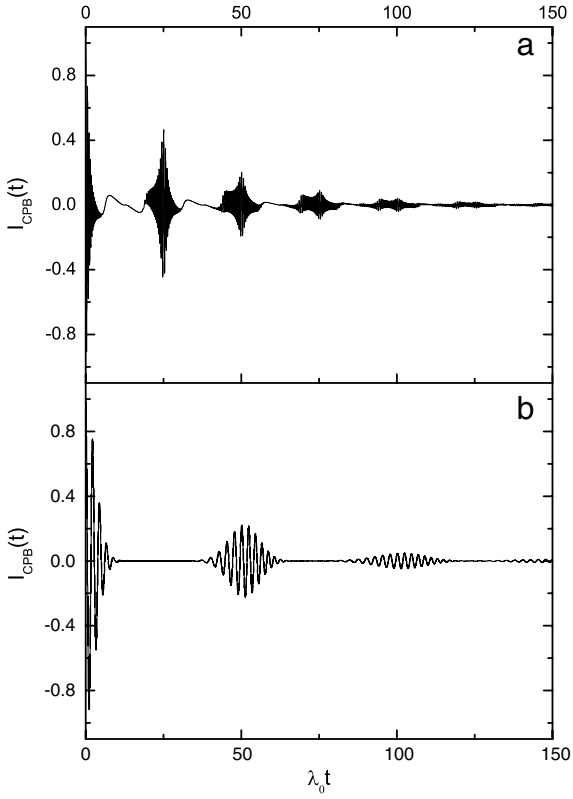

Fig. 10. Same as in Figs. 8 and 9, for time dependent detunings (cf. $f(t) = c\sin(\omega' t)$): (a) $c = 20\lambda_0, \omega' = 0.5\lambda_0$, (b) $c = 60\lambda_0, \omega' = 20\lambda_0$, with $\alpha = 5, \omega = \omega_0 = 2000\lambda_0, \gamma = 0.05\lambda_0$.

values of the associated parameters. We have included dissipation and assumed the CPB in excited state and the NR initially in a SC state (see generation in Ref. [65]). We have also considered the following scenarios: (i) resonant case (detuning $f = 0$); (ii) off-resonant case, with a constant detuning ($f = \Delta \neq 0$), and (iii) off-resonant case, with a time dependent detuning ($f(t) = c\sin(\omega' t)$). The results were discussed in the previous section. Concerning with the entropy we see that when the NR is initially in a "Schrödinger-cat" state, the entropy lasts longer than in an atom–field system with the field initially in a coherent state (cf. Ref. [31]). Concerning with the excitation inversion, an interesting result emerges: although the presence of a constant detuning destroys the collapse and revivals of the excitation inversion, these effects are restituted by the action of convenient time dependent detunings—even in the presence of damping. Finally, it is worth emphasizing that external forces acting upon the NR originate from the changes in the magnetic flux Φ_e (cf. Fig. 1), which provide the control of the parameters $\omega(t)$ and $\lambda(t)$.

Acknowledgments

The authors thank the FAPEG (CV) and CNPq (ATA, BB), Brazilian Agencies, for partially supporting this work.

References

[1] H.J. Carmichael, D.F. Walls, J. Phys. B: At. Mol. Phys. 9 (1976) L43–L46.
[2] H.J. Kimble, M. Dagenais, L. Mandel, Phys. Rev. Lett. 39 (1977) 691–695.
[3] R.E. Slusher, L.W. Hollberg, B. Yurke, J.C. Mertz, J.F. Valley, Phys. Rev. Lett. 55 (1985) 2409–2412.
[4] D. Stoler, Phys. Rev. D 1 (1970) 3217–3219.
[5] G. Rempe, H. Walther, N. Kelein, Phys. Rev. Lett. 58 (1990) 353–356.
[6] B. Yurke, D. Stoler, Phys. Rev. Lett. 57 (1986) 13–16.
[7] M. Brune, S. Haroche, J.M. Raimond, L. Davidovich, N. Zagury, Phys. Rev. A 45 (1992) 5193–5214.
[8] M. Brune, E. Hagley, J. Dreyer, X. Mai'tre, A. Maali, C. Wunderlich, J.M. Raimond, S. Haroche, Phys. Rev. Lett. 77 (1996) 4887–4890.
[9] C. Monroe, D.M. Meekhof, B.E. King, D.J. Wineland, Science 272 (1996) 1131–1136.
[10] C.H. Bernnett, G. Brassard, C. Crépeau, R. Jozsa, A. Peres, W.K. Wootters, Phys. Rev. Lett. 70 (1993) 1895–1899.
[11] A. Einstein, B. Podolsky, N. Rosen, Phys. Rev. A 47 (1935) 777–780.
[12] D. Bouwmeester, J.W. Pan, K. Mattle, M. Eibl, H. Weinfurter, A. Zeillinger, Nature 390 (1997) 575–579.
[13] B. Julsgaard, A. Kozhekin, E.S. Polzik, Nature 413 (2001) 400–403.
[14] J.I. Cirac, A.S. Parkins, Phys. Rev. A 50 (1994) 4441–4444.
[15] M.H.Y. Moussa, Phys. Rev. A 55 (1997) R3287–R3290.

[16] M.H.Y. Moussa, B. Baseia, Modern Phys. Lett. B 12 (1998) 1209–1212.
[17] D. Boschi, S. Branca, F.D. Martini, L. Hardy, S. Popescu, Phys. Rev. Lett. 80 (1998) 1121–1125.
[18] C. Valverde, B. Baseia, Int. J. Quantum Inf. 2 (2004) 421–445.
[19] G. Rempe, M.O. Scully, H. Walther, Phys. Scr. T34 (1991) 5–13.
[20] J.M.C. Malbouisson, B. Baseia, Phys. Lett. A 290 (2001) 234–238.
[21] C. Valverde, A.T. Avelar, B. Baseia, J.M.C. Malbouisson, Phys. Lett. A 315 (2003) 213–218.
[22] J.M. Raymond, M. Brune, S. Haroche, Rev. Modern Phys. 73 (2001) 565, and references their in.
[23] A.I. Lvovsky, S.A. Barvichev, Phys. Rev. A 66 (2002) 011801R.
[24] Y. Guimarães, B. Baseia, C.J. Villas-Boas, M.H.Y. Moussa, Phys. Lett. A 268 (2000) 260–267.
[25] C.J. Villas-Boas, Y. Guimarães, M. Moussa, B. Baseia, Phys. Rev. A 63 (2001) 055801.
[26] W. Paul, Rev. Modern Phys. 62 (1990) 531–540.
[27] H. Dehmelt, Rev. Modern Phys. 62 (1990) 525–530.
[28] C.K. Law, S.Y. Zhu, M.S. Zubairy, Phys. Rev. A 52 (1995) 4095–4098.
[29] M. Janowicz, Phys. Rev. A 57 (1998) 4784–4790.
[30] G.F. Zhang, X.C. Xie, Eur. Phys. J. D 60 (2010) 423–427.
[31] J. Fei, S.Y. Xie, Y.P. Yang, Chin. Phys. Lett. 27 (2010) 014212.
[32] M.S. Ateto, Internat. J. Theoret. Phys. 49 (2010) 276–292.
[33] M.S. Abdalla, M. Abdel-Aty, A.S.F. Obada, Physica A 326 (2003) 203–219.
[34] A. Olaya-Castro, N.F. Johnson, L. Quiroga, Phys. Rev. A 70 (2004) 020301.
[35] Y.P. Yang, J.P. Xu, G.X. Li, H. Chen, Phys. Rev. A 69 (2004) 053406.
[36] O. Astafiev, Y.A. Pashkin, Y. Nakamura, T. Yamamoto, J.S. Tsai, Phys. Rev. Lett. 93 (2004) 267007.
[37] R. Ruskov, K. Schwab, A.N. Korotkov, Phys. Rev. B 71 (2005) 235407.
[38] E.K. Irish1, K. Schwab, Phys. Rev. B 68 (2003) 155311.
[39] J. Siewert, T. Brandes, G. Falci, Phys. Rev. B 79 (2009) 024504.
[40] C.P. Sun, L.F. Wei, Y. Liu, F. Nori, Phys. Rev. A 73 (2006) 022318.
[41] J. Liao, Q. Wu, L. Kuang, 2008. arXiv:quant-ph/0803.4317v1.
[42] S. Brattke, B.T.H. Varcoe, H. Walther, Phys. Rev. Lett. 86 (2001) 3534–3537.
[43] Y. Liu, L.F. Wei, F. Nori, Phys. Rev. A 71 (2005) 063820.
[44] X.X. Zhou, A. Mizel, Phys. Rev. Lett. 97 (2006) 267201.
[45] G. Chen, Z. Chen, L. Yu, J. Liang, Phys. Rev. A 76 (2007) 024301.
[46] L.F. Wei, Y. Liu, F. Nori, Phys. Rev. Lett. 96 (2006) 246803.
[47] L. Avijit, 2003. arXiv:quant-ph/0302029v2.
[48] L. Avijit, N. Sankhasubhra, Phys. Lett. A 318 (2003) 6.
[49] J.N. Bandyopadhyay, A. Lakshminarayan, Phys. Rev. Lett. 89 (2002) 060402.
[50] A. Lakshminarayan, V. Subrahmanyam, 2002. arXiv: quant-ph/0212049v2.
[51] M.O. Scully, M.S. Zubairy, Quantum Optics, Cambridge University Press, Cambridge, 1997, 195.
[52] M.O. Scully, M.S. Zubairy, Quantum Optics, Cambridge University, Cambridge, 1997, pp. 136–195.
[53] H.G. Baker, R.L. Singleton, Phys. Rev. A 42 (1990) 10–17.
[54] J.C. Lemm, B.G. Giraud, A. Weiguny, Phys. Rev. Lett. 73 (1994) 420–423.
[55] H. Lee, W.S. I'yi, Phys. Rev. A 51 (1995) 982–988.
[56] P.M. Visser, G. Nienhuis, Phys. Rev. A 52 (1995) 4727–4736.
[57] K. Belharaya, P. Blaise, O.H. Rousseau, Chem. Phys. 293 (2003) 9–22.
[58] C.F.M. Faria, A. Fring, Laser Phys. 17 (2007) 424–437.
[59] S.G. Rajeev, Ann. Phys. 322 (2007) 1541–1555.
[60] P.R. Giri, P. Roy, Eur. Phys. J. C 60 (2009) 157–161.
[61] S. Longhi, Phys. Rev. Lett. 105 (2010) 013903.
[62] Q. Yang, M. Yang, Z.L. Cao, Chin. Phys. Lett. 26 (2009) 040302.
[63] W.C. Qiang, W.B. Cardoso, X.H. Zhanga, Physica A 389 (2010) 5109.
[64] S.J.D. Phoenix, P.L. Knight, Phys. Rev. A 44 (1991) 6023.
[65] L. Tian, Phys. Rev. B 72 (2005) 195411.